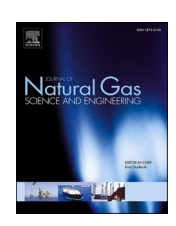
ELSEVIER

Contents lists available at ScienceDirect

Journal of Natural Gas Science and Engineering

journal homepage: http://www.elsevier.com/locate/jngse





Numerical study of the effect of propped surface area and fracture conductivity on shale gas production: Application for multi-size proppant pumping schedule design

Parth Bhandakkar a,b, Prashanth Siddhamshetty a,b, Joseph Sang-Il Kwon a,b,*

- ^a Artie McFerrin Department of Chemical Engineering, Texas A&M University, College Station, TX 77845, USA
- b Texas A&M Energy Institute, Texas A&M University, College Station, TX 77845, USA

ARTICLE INFO

Keywords: Multi-size proppant pumping schedule Hydraulic fracturing Unconventional reservoirs Optimization Reduced order modeling Neural network

ABSTRACT

Hydraulic fracturing is a technique extensively used in the oil and gas industry, where water, proppant (sand) and additives are injected into unconventional reservoirs to enhance the recovery of shale hydrocarbon. Although some previous studies have developed pumping schedules that maximize gas production for a singlesize proppant, there are very few studies that consider the effect of varying proppant diameters across pumping stages on shale gas production. Motivated by this, we carried out an extensive sensitivity analysis to determine the effect of different proppant diameters on the average fracture conductivity (FC), average propped surface area (PSA) and cumulative shale gas production volume. We found out that the cumulative shale gas production volume depends on both the average PSA and average FC. We also found out that small-diameter proppant resulted in higher average PSA and lower average FC, whereas large-diameter proppant resulted in lower average PSA and higher average FC. Hence, we designed a multi-size proppant pumping schedule considering both of these parameters into account for simultaneously propagating multiple fractures to maximize shale gas production from unconventional reservoirs. Since the size of injected proppant particles determines the average PSA and average FC for the propped hydraulic fractures, we developed a novel framework called Sequentially Interlinked Modeling Structure (SIMS) to predict the average PSA, average FC and cumulative shale gas production volume at the end of 10 years for a given pumping schedule. Then, we used this SIMS framework to obtain a multi-size proppant pumping schedule that maximizes shale gas production. Finally, we demonstrated that the obtained pumping schedule gives a cumulative shale gas production volume greater than the values obtained from the existing pumping schedules.

1. Introduction

Hydraulic fracturing is a stimulation technique to enhance the oil and gas production that typically involves injecting water, proppant (sand), and additives under high pressure into unconventional reservoirs. Hydraulic fracturing, commonly known as 'fracking', is used to create new fractures in the existing rock, and also increase the size, spread, connectivity and conductivity of existing fractures. This technique is commonly used in low-permeability rocks like shale and tight sandstone to increase oil and/or gas flow to a well from petroleum-bearing unconventional reservoirs. The importance of using proppant in the hydraulic fracturing operation in unconventional reservoirs has been discussed in detail by Fredd et al. (2000).

In the hydraulic fracturing operation for unconventional reservoirs, it is important to achieve an optimal fracture geometry to maximize the gas production (Siddhamshetty et al., 2017). Lately, researchers have developed model-based feedback control strategies to achieve an optimal fracture geometry (Narasingam et al., 2017, 2018; Gu and Hoo, 2014; Sidhu et al., 2018a, b; Siddhamshetty et al., 2017, 2018a, 2018b, 2019; Siddhamshetty and Kwon, 2019; Siddhamshetty et al., 2020; Yang et al., 2017; Westwood et al., 2017). However, they used a single-size proppant to design pumping schedules.

For determining the oil and gas production from unconventional reservoirs, average propped surface area (PSA) and average fracture conductivity (FC) of the propped hydraulic fractures play an important role. Average PSA and average FC depend largely on the injected

^{*} Corresponding author. Artie McFerrin Department of Chemical Engineering, Texas A&M University, College Station, TX 77845, USA. E-mail address: kwonx075@tamu.edu (J. Sang-Il Kwon).

proppant diameter. Existing studies on average PSA or average FC considered these two effects separately, and did not consider their combined effect on shale gas production. Wahl (1965) discussed, for the first time, the importance of effective total fracture surface area (TFSA), instead of TFSA, for horizontal fractures, and developed a new technique to maximize the effective TFSA. Ramurthy et al. (2011) elaborated in detail that different shale plays require different types of treatment, either maximizing surface area or conductivity. They also presented tests like Brinell Hardness Test and Diagnostic Fracture Injection Test to determine the type of treatment required for the sample reservoir being tested. Schmidt et al. (2014) have done an extensive study on a laboratory scale to understand the impact of multi-size proppant addition on FC. Hu et al. (2018) further discussed a multi-size proppant pumping schedule in a pre-existing straight fracture on a laboratory scale. Specifically, their objective was to transport proppant deeper into the fracture, instead of considering PSA or FC to quantify shale gas production from unconventional reservoirs. Motivated by these considerations, in this work, we developed a framework called Sequentially Interlinked Modeling Structure (SIMS) to relate average PSA, average FC, and cumulative shale gas production volume from an unconventional reservoir, when a multi-size proppant pumping schedule is introduced to simultaneously propagating multiple fractures. We further integrated the SIMS framework to obtain a multi-size proppant pumping schedule that maximizes the cumulative shale gas production volume in unconventional reservoirs.

This paper is structured as follows: In Section 2, the use of Petrel as a high-fidelity model to simulate simultaneously propagating multiple fractures is described. In Section 3, the effect of changing proppant sizes during the hydraulic fracturing process is presented. In Section 4, we present an overview of SIMS, the novel framework proposed in this work. Next, in Section 5, we propose an optimization problem using the proposed SIMS framework, with the constraints on fracturing fluid flow rate, proppant concentration and proppant sizes available for injection, to obtain pumping schedules that maximize shale gas production from unconventional reservoirs. Finally, in Section 6, results showing that the obtained pumping schedule leads to the maximum cumulative shale gas production from an unconventional reservoir, considering simultaneously propagating multiple fractures, are presented. We also present a comparison of the obtained pumping schedule with the existing pumping schedules, to show that the obtained pumping schedule leads to an increase in the cumulative shale gas production volume.

2. High-fidelity model

This section discusses the Unconventional Fracture Model (UFM) developed by Weng et al. (2014). In this work, it has been used as a high-fidelity simulator for modeling simultaneously propagating multiple fractures in an unconventional reservoir. Next, we will discuss the reservoir simulator used in this work to model shale gas production.

2.1. Basics of the UFM

The UFM solves equations in which rock deformation and fluid flow are coupled, which is very similar to that of P3D model (Weng et al., 2014). The UFM mainly stands out from other hydraulic fracture models

in the sense that it also considers the stress-shadow interactions between nearby fractures. This enables the model to accurately predict the path of fracture propagation, especially when narrowly-spaced multiple hydraulic fractures are being simultaneously propagated. The UFM solves a system of coupled equations describing fracture deformation, height growth, fracturing fluid flow, conservation of mass, proppant transport and fracture interaction for simultaneously propagating multiple fractures, which is described below in further detail.

2.1.1. Fluid flow equations

For simultaneously propagating multiple fractures, the local mass conservation equation is as follows:

$$\frac{\partial q}{\partial s} + \frac{\partial (H_{fl}\overline{w})}{\partial t} + q_L = 0 \tag{1}$$

$$q_L = 2h_L u_L \tag{2}$$

where \overline{w} denotes the average fracture width at position s=s(x,y), q is the local fracturing fluid flow rate, H_{fl} denotes the fracture height at location s and time t, q_L is the volumetric rate leaking off through the fracture wall, and u_L is the leak-off velocity. It is worthwhile to note that Carter's leak-off model is used to calculate the leak-off term in this work.

Poiseuille law is used to describe the pressure drop along a fracture branch for laminar flow, assuming it as a power-law fluid, which is described as follows:

$$\frac{\partial p}{\partial s} = -\alpha_0 \frac{1}{\overline{w}^{2n'+1}} \frac{q}{H_{fl}} \left| \frac{q}{H_{fl}} \right|^{n'-1} \tag{3a}$$

and the pressure drop for turbulent flow is as follows:

$$\frac{\partial p}{\partial s} = -\frac{f\rho}{\overline{w}^3} \frac{q}{H_g} \left| \frac{q}{H_g} \right| \tag{3b}$$

where

$$\alpha_0 = \frac{2k^{\cdot}}{\varphi(n^{\cdot})^n} \cdot \left(\frac{4n^{\cdot} + 2}{n^{\cdot}}\right)^{n^{\cdot}}; \ \varphi(n^{\cdot}) = \frac{1}{H_{fl}} \int_{H_{fl}} \left(\frac{w(z)}{\overline{w}}\right)^{\frac{2n^{\cdot} + 1}{n}} dz \tag{4}$$

where w(z) is the fracture width as a function of depth z, p denotes the fluid pressure, ρ represents the slurry density, f is the fanning factor, and n' and k' are the power-law index and consistency index, respectively, for the fracturing fluid.

In rock formations, the fracture toughness, elastic modulus, in-situ stresses, fluid pressure and thickness of each layer govern the width and height of propagating fractures. At the fracture tips, fracture toughness is matched to the stress intensity factors for the calculation of fracture height. Mack et al. (1992) states these stress intensity factors and width profile as follows:

$$K_{1l} = \sqrt{\frac{\pi h}{2}} \left[p_{cp} - \sigma_n + \rho_f g \left(h_{cp} - \frac{h}{4} \right) \right] + \sqrt{\frac{2}{\pi h}} \sum_{i=1}^{n-1} (\sigma_{i+1} - \sigma_i) \times \left[\frac{h}{2} \arccos \left(\frac{h - 2h_i}{h} \right) + \sqrt{h_i (h - h_i)} \right]$$
(5a)

$$K_{1u} = \sqrt{\frac{\pi h}{2}} \left[p_{cp} - \sigma_n + \rho_f g \left(h_{cp} - \frac{3h}{4} \right) \right] + \sqrt{\frac{2}{\pi h}} \sum_{i=1}^{n-1} (\sigma_{i+1} - \sigma_i) \times \left[\frac{h}{2} \arccos \left(\frac{h - 2h_i}{h} \right) + \sqrt{h_i (h - h_i)} \right]$$
(5b)

$$w(z) = \frac{4}{E'} \left[p_{cp} - \sigma_n + \rho_f g \left(h_{cp} - \frac{h}{4} - \frac{z}{2} \right) \right] \sqrt{z(h-z)} + \frac{4}{\pi E'} \sum_{i=1}^{n-1} (\sigma_{i+1} - \sigma_i) \left[(h_i - z) \operatorname{arcCosh} \frac{z \left(\frac{h-2h_i}{h} \right) + h_i}{|z - h_i|} + \sqrt{z(h-z)} \operatorname{arccos} \left(\frac{h-2h_i}{h} \right) \right]$$

$$(5c)$$

where K_{1l} and K_{1u} denote the stress intensity factors at the bottom and top of fracture tips, respectively, p_{cp} denotes the pressure of the fracturing fluid measured at a height h_{cp} for the reference fracture, h represents the fracture height, h_i denotes the distance between the top of i^{th} layer and the fracture bottom tip, σ_n and σ_i are the in-situ stresses at the top and the i^{th} layer, respectively, and ρ_f denotes the fluid density. In $E' = E/(1-\nu^2)$, E represents Young's modulus, and ν represents Poisson's ratio

Moreover, at every time instant, a global volume balance equation is solved as follows:

$$\int_{0}^{t} Q(t)dt^{*} = \int_{0}^{L(t)} h(s,t)\overline{w}(s,t)ds + \int_{H_{L}} \int_{0}^{t} \int_{0}^{L(t)} 2u_{L}dsdt^{*}dh_{L}$$
 (6)

where t denotes the current time, Q(t) denotes the fracturing fluid flow rate at the wellbore, and L(t) is the total length of the fracture at time t. A qualitative equivalence of this equation is that the total amount of fluid injected in the hydraulic fracturing process is equal to the amount present in the fractures and the amount that has leaked-off into the nearby formation

Along with the boundary conditions that state zero width, zero net pressure and zero flow rate at the fracture tip, the equations stated above describe the fluid flow through simultaneously propagating multiple fractures.

2.1.2. Stress shadow effects

The presence of multiple fractures near the hydraulic fracture can cause a significant perturbation to its propagation path. This phenomenon is known as the stress shadow effect. We have used 2D Displacement Discontinuity Method (DDM) (Crouch et al., 1983) to calculate the shear and normal stresses acting on a fracture element due to shearing and normal displacement discontinuities. The stresses can be calculated using the following equations:

$$\sigma_s^i = \sum_{j=1}^N A^{ij} C_{ss}^{ij} D_s^j + \sum_{j=1}^N A^{ij} C_{sn}^{ij} D_n^j$$
 (7a)

$$\sigma_n^i = \sum_{i=1}^N A^{ij} C_{ns}^{ij} D_s^i + \sum_{i=1}^N A^{ij} C_{nn}^{ij} D_n^i$$
(7b)

where σ_s and σ_n denote the shear and normal stresses, respectively, A^{ij} denotes 3D correction factors to consider the effect caused by a finite fracture height (Olson, 2008), C^{ij} denotes 2D plane-strain elastic influence coefficients, and D_s and D_n are the shearing and opening displacement discontinuities, respectively.

By taking into account these equations, Schlumberger has

successfully developed an extensive hydraulic fracturing simulator called 'Mangrove', which is based on UFM. Mangrove is available in the Schlumberger Petrel platform, which has been used in this work as a virtual experiment (i.e., high-fidelity model) to simulate fracture propagation, fluid flow and proppant transport in the case of simultaneously propagating multiple fractures.

Remark 1. Thickness of the reservoir, Poisson ratio, Young's modulus, maximum and minimum horizontal stresses are a few initiation parameters needed to be specified in Mangrove for the given rock formation. In practice, wellbore failure image and extended leak-off test can be used to determine the maximum and minimum horizontal stresses, respectively, and well logs can be used to quantify elastic properties like Young's modulus and Poisson ratio.

2.2. Reservoir simulator

Once fracture propagation, fluid flow, and proppant transport and settling have been modeled in Mangrove, Petrel has been used again to model shale gas production from an unconventional reservoir, stimulated using simultaneously propagating multiple fractures. The output from the UFM is fed as an input to the automated grid generator (Cipolla et al., 2011). After this production grid is generated, we simulate shale gas production from a well in an unconventional reservoir using INTERSECT reservoir simulator.

3. Sensitivity analysis to understand the effect of varying proppant size during injection

In this section, we present a sensitivity analysis result showing the effect of changing proppant size on average PSA and average FC in simultaneously propagating multiple fractures. For this analysis, we have used 0.0065 inch and 0.04 inch proppant particles.

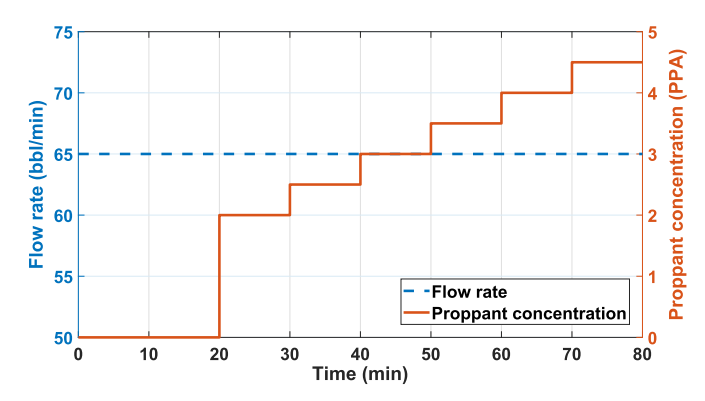


Fig. 1. Pumping schedule considered in the sensitivity analysis.

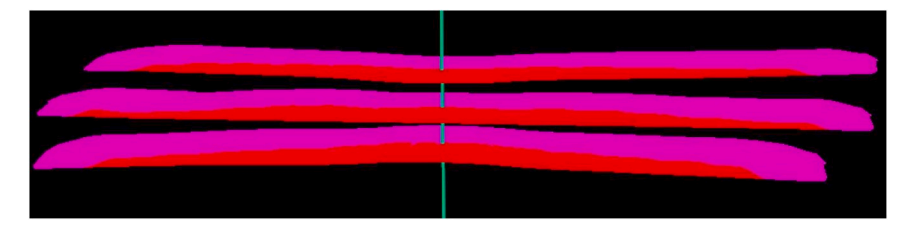


Fig. 2. Post-settling proppant distribution in Case 1.

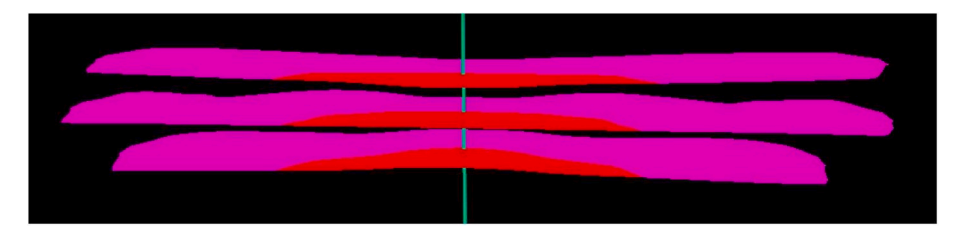


Fig. 3. Post-settling proppant distribution in Case 2.

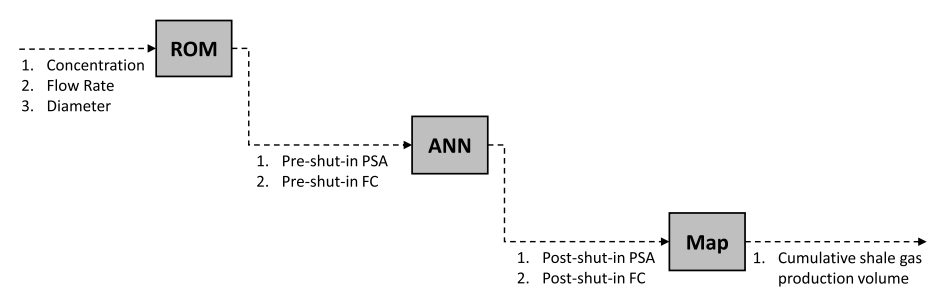


Fig. 4. Illustration showing the proposed SIMS framework.

Two pumping schedules, which have similar pumping flow rates and concentration profiles but different proppant sizes, were considered in this case, as shown in Fig. 1.

These pumping schedules were subsequently used in the UFM to simulate simultaneously propagating multiple fractures and subsequent gas production. Specifically, the first pumping schedule uses only a small-diameter proppant (Case 1), whereas the other includes only a large-diameter proppant (Case 2). For Case 1, we found the average PSA and the average FC at the end of the settling process to be 429780.32 $\rm ft^2$ and 199.71 mD·ft, respectively. For Case 2, we found the average PSA and average FC at the end of the settling process to be 241760.67 $\rm ft^2$ and 17619.81 mD·ft, respectively. The cumulative shale gas production

volumes at the end of 30 years in these cases are 368997.94 MSCF and 362948.94 MSCF, respectively. Fig. 2 and Fig. 3 show the post-settling fracture geometry qualitatively. In the figures, the settled proppant banks are in red, and the unpropped hydraulic fractures are in pink. The figures clearly show that in Case 1, the proppant bank is longer and has penetrated deeper into the fracture than Case 2.

From the sensitivity analysis, we can conclude a few things: First, average PSA is greater in Case 1 than Case 2. This is primarily because smaller proppant particles tend to suspend in the fracturing fluid for longer times, and hence, can penetrate deeper along the fracture length. Second, average FC in Case 2 is more than Case 1. This is clearly because large proppant particles has high permeability, which directly translates

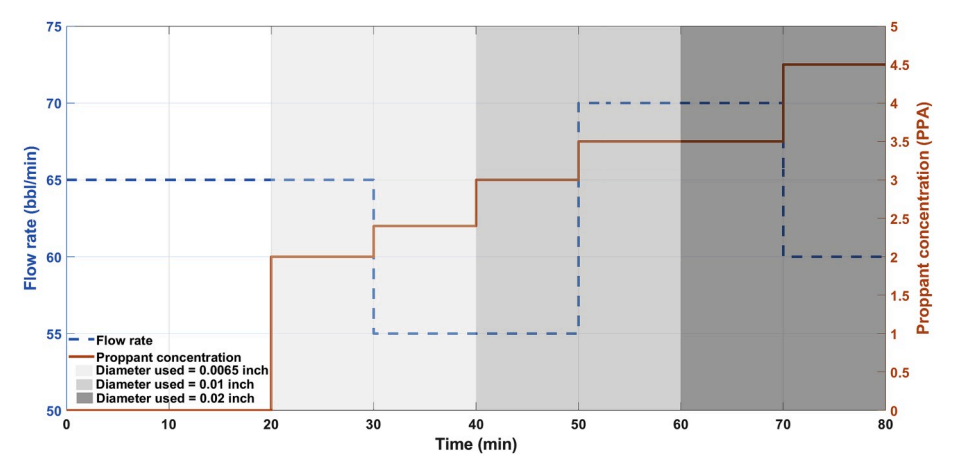


Fig. 5. The pumping schedule used for training Model 1 (MOESP-based ROM).

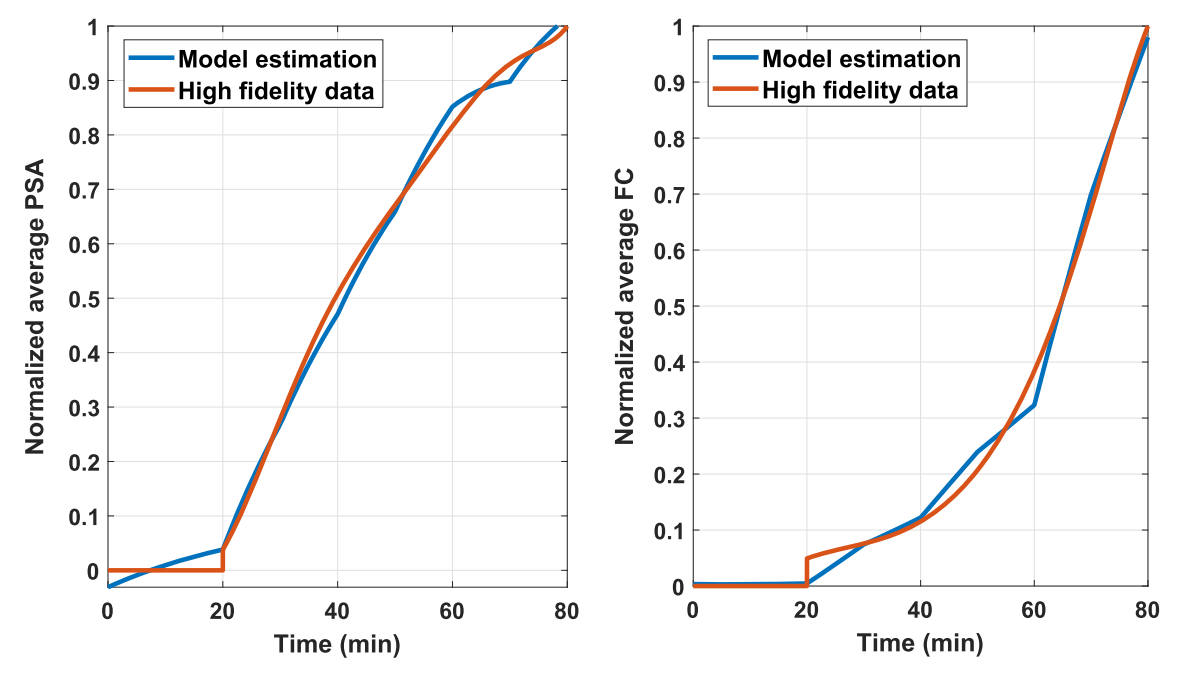


Fig. 6. Training fit for Model 1 (MOESP-based ROM).

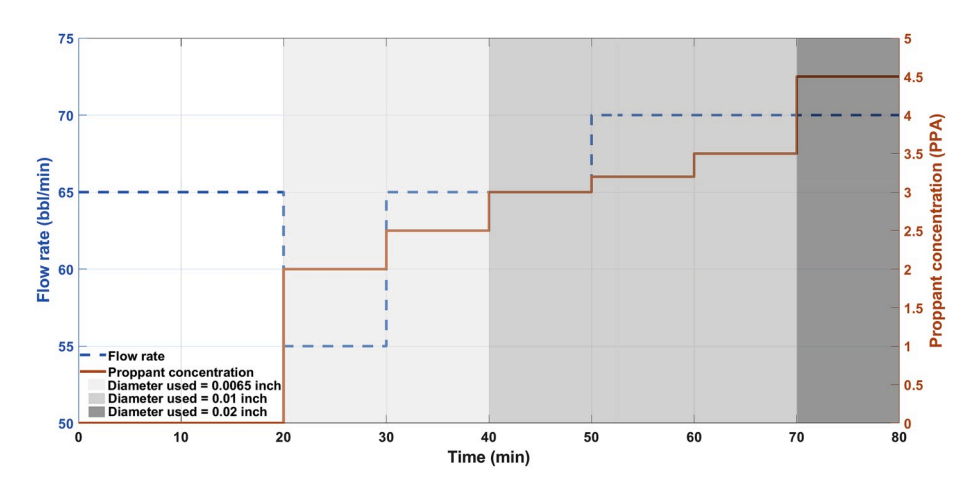


Fig. 7. The pumping schedule used for validating Model 1 (MOESP-based ROM).

to high average FC of the propped fractures. Third, the cumulative shale gas production volume is almost similar in both the cases. This stems from the fact that we can not rely only on either the average PSA or the average FC separately to accurately predict the shale gas production volume. Instead, there is a dependence of the cumulative gas production volume on both of these parameters, as is visible from the sensitivity analysis.

Motivated by this observation, we propose a new framework in the following section to determine the cumulative shale gas production volume for a given pumping schedule. Then, the proposed model will be further used to obtain pumping schedules to maximize the cumulative shale gas production volume from unconventional reservoirs.

4. Proposed SIMS framework

In this paper, a framework called SIMS is proposed to describe the cumulative shale gas production volume from simultaneously propagating multiple fractures. This approach has two major advantages, as compared to a model that directly correlates the cumulative shale gas production volume from pumping schedules. First, it provides more

insight into the process of hydraulic fracturing by breaking it down into smaller parts. An integrated framework having multiple models is easier to comprehend than a single model capturing the fracture propagation, proppant settling and gas production dynamics for an unconventional reservoir. Second, this approach also provides us with average PSA and average FC in the intermediate step after the hydraulic fracturing operation that typically takes a few hours. These parameters are usually of practical importance to the oil and gas industries, instead of just the cumulative shale gas production volume at the end of 10 years.

In this work, we have incorporated three models into the proposed SIMS framework. The first model is an MOESP-based ROM of the fracturing process. The second model is an Artificial Neural Network (ANN) that has been used to accurately simulate the gravity-induced proppant settling process. The third model is a map that links the average PSA and the average FC of the created hydraulic fractures to the cumulative shale gas production volume from an unconventional reservoir. These models are interlinked in the sense that the output from the first model is the input to the second, and the output from the second model is the input to the third. A simplified design of the SIMS framework is shown in Fig. 4.

The following subsections further elaborate each of these three

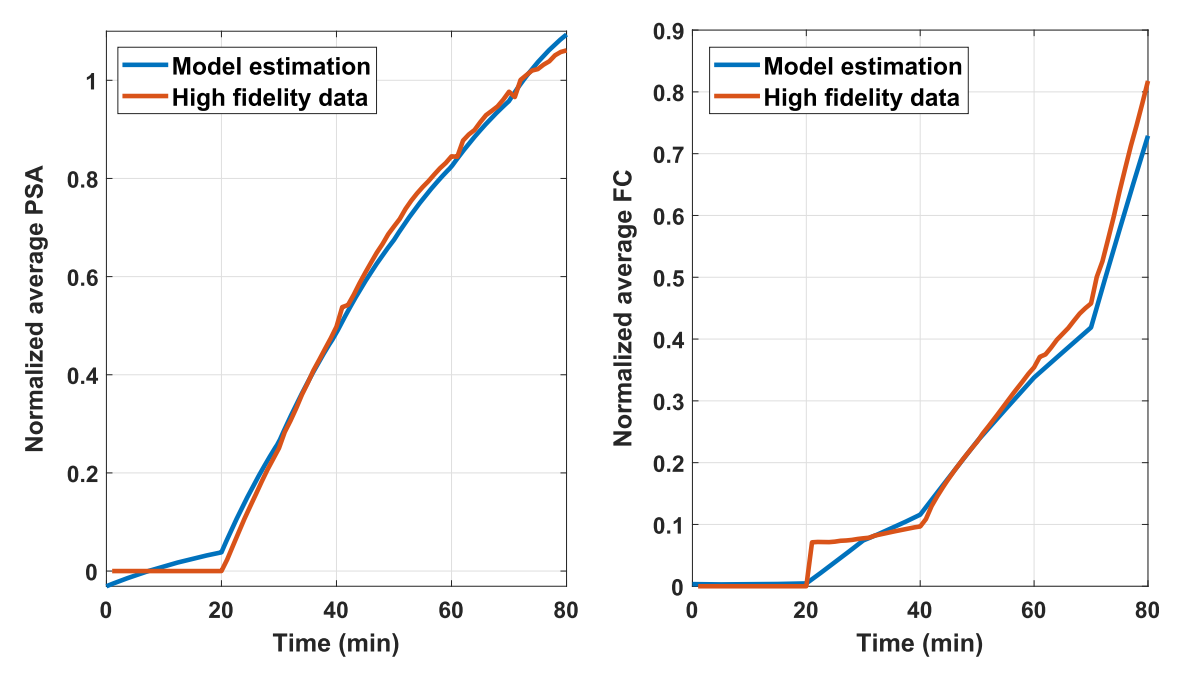


Fig. 8. Validation fit for Model 1 (MOESP-based ROM).

models in detail.

4.1. Model 1: MOESP-based ROM to simulate hydraulic fracturing

Since it is computationally infeasible to directly use the UFM, Eqs. (1)–(7), we developed an MOESP-based ROM to describe the propagation, fluid flow and proppant transport phenomena for simultaneously propagating multiple fractures, which is given below:

$$x(t_{k+1}) = Ax(t_k) + Bu(t_k)$$
 (8a)

$$y(t_k) = Cx(t_k) \tag{8b}$$

where $x(t_k)$ are the ROM states, $u(t_k) = [Q_{x0}(t_k), C_{x0}(t_k), D_{x0}(t_k)]^T$ represent the input variables, $Q_{x0}(t_k)$, $C_{x0}(t_k)$ and $D_{x0}(t_k)$ are the fracturing fluid flow rate, proppant concentration and the injected proppant diameter, respectively, and the output variables, $y(t_k) = [PSA_{frac}(t_k), Conductivity_{frac}(t_k)]^T$, are the average PSA and average FC at the end of pumping. It is worthwhile to note that this model is only used to describe the hydraulic fracturing process until the end of pumping (i.e., pre-shutin). Other data-based techniques can be also used to derive computationally more efficient models (Narasingam and Kwon, 2017, 2018).

A training data set has been used to obtain the model parameters to be determined (i.e., x(0), the initial estimate of the state, and the matrices A, B, and C) for a given order of the MOESP algorithm. Openloop simulations were carried out using Mangrove and the data were used to create a 2^{nd} order linear time-invariant state-space model. The pumping schedule chosen for training the ROM is shown in Fig. 5.

This training input is chosen such that it satisfies the minimum and maximum practical fracturing fluid flow rate and proppant concentration. The proppant diameters chosen in the training input pumping schedule are also ensured to follow a non-decreasing trend across the pumping stages, which is a common industry practice. Fig. 6 shows the training fit between the estimated average PSA and average FC values from the MOESP-based ROM and the corresponding values from Mangrove (i.e., high-fidelity model).

It is observed that the estimated average PSA and average FC converge quickly to the true values. The computational effort required to solve Eq. (8) is very small as compared to that of solving the UFM, Eqs. (1)–(7). The performance of the ROM has been validated by comparing

it with a different testing pumping schedule within the practical considerations (Fig. 7).

Fig. 8 shows the comparison between the ROM and Mangrove. It can be clearly seen that the average PSA and average FC obtained from the ROM are close to the corresponding outputs obtained from Mangrove.

4.2. Model 2: ANN-based model to simulate proppant settling

The second model in the SIMS framework is an ANN. This is an inputoutput model to capture the proppant settling dynamics in simultaneously propagating multiple fractures. At the end of pumping (i.e., preshut-in stage), the proppant in suspension starts settling down due to gravity. When the dynamic settling process has finally completed and reached an equilibrium (i.e., post-shut-in stage), a proppant bank is formed in the propped hydraulic fractures. This model takes the preshut-in average PSA and pre-shut-in average FC predicted from Model 1 as the two inputs and provides the post-shut-in average PSA and postshut-in average FC of the propped hydraulic fractures as the two outputs. The input-output data required for developing this model were collected using Schiller and Naumann correlation available in Mangrove as the principle for capturing proppant settling (Schiller and Naumann, 1935; Daneshy, 1978). The network structure is designed to have two hidden layers, with two nodes in each hidden layer. This model is intermediate as it takes its inputs from Model 1 and passes on its outputs to Model 3, hence acting as a bridge between the other two models. A simplified illustration of the structure is shown in Fig. 9.

These training inputs and training outputs have been obtained by applying several different pumping schedules of a variety of proppant diameters, flow rates and concentrations to the UFM. The network has then been trained using Baysian Regularization method with sigmoidal activation functions. Specifically, 110 samples were used for training the network. Scatter-fit for the training samples for the proposed network can be seen from Fig. 10.

The trained ANN is then used to test 25 samples, which were not used during the training process. When this trained network was used on the test samples, the corresponding mean squared error (MSE) value was found to be 0.0045, which indicates a well-trained model. The scatter fit for the testing samples can be seen from Fig. 11.

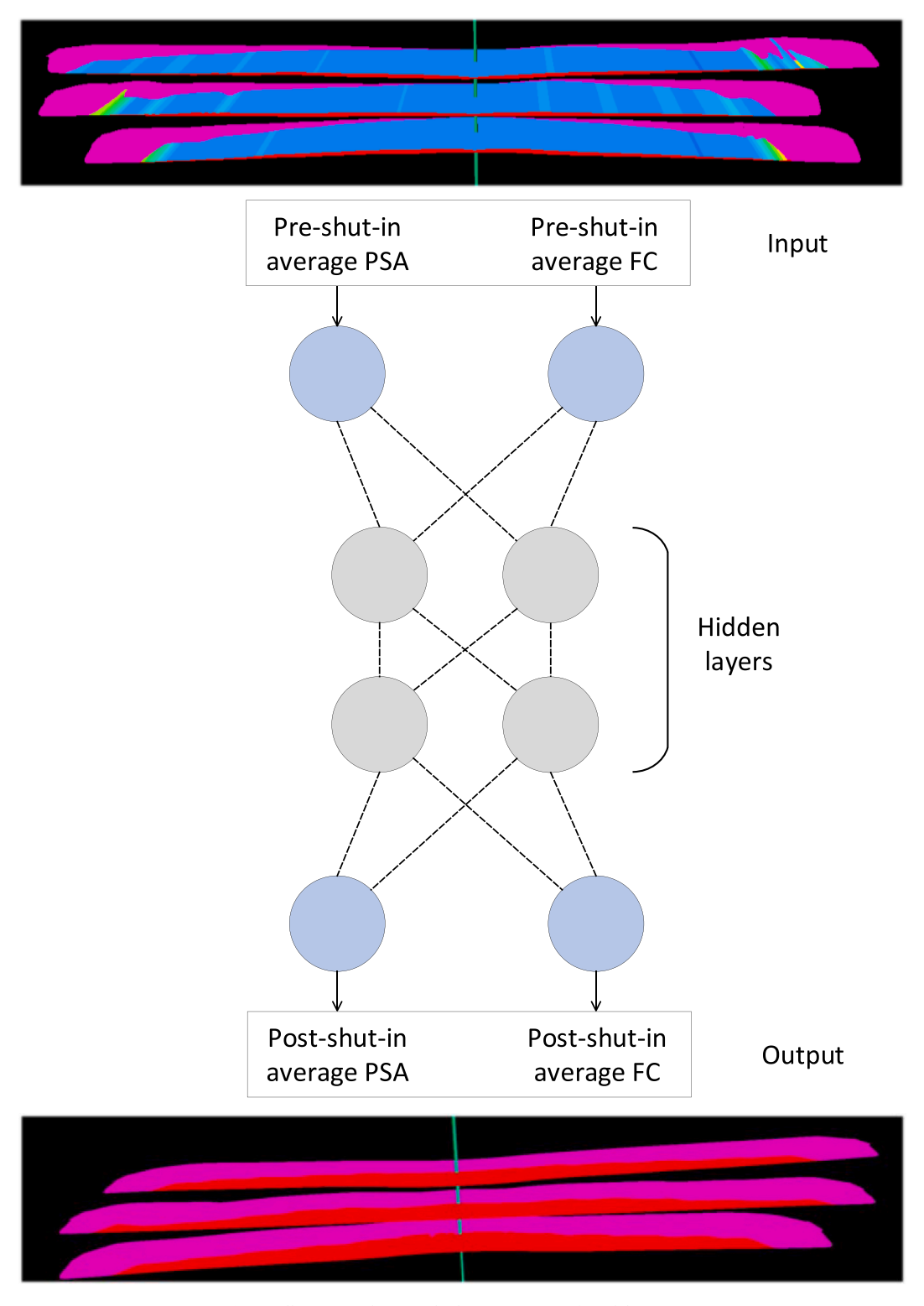


Fig. 9. Illustration showing the basic structure of Model 2 (ANN).

The third model in SIMS framework is a map that has been generated using UFM (Mangrove) and INTERSECT Production Simulator. It has been generated using 86 pumping schedules, with varying proppant concentration, fluid flow rates and proppant diameters. The model is based on the assumption that the cumulative shale gas production

volume from an unconventional reservoir depends only on the average PSA and the average FC of propped fractures. The map is shown in Fig. 12. The x-axis in the map corresponds to average FC and the y-axis corresponds to the average PSA. The z-axis of the map denotes the cumulative amount of shale gas produced from the reservoir at the end of 10 years. It is worthwhile to note that since this final map linking propped fracture properties to the cumulative shale gas production volume is non-monotonic in nature, we proceeded with formulating an

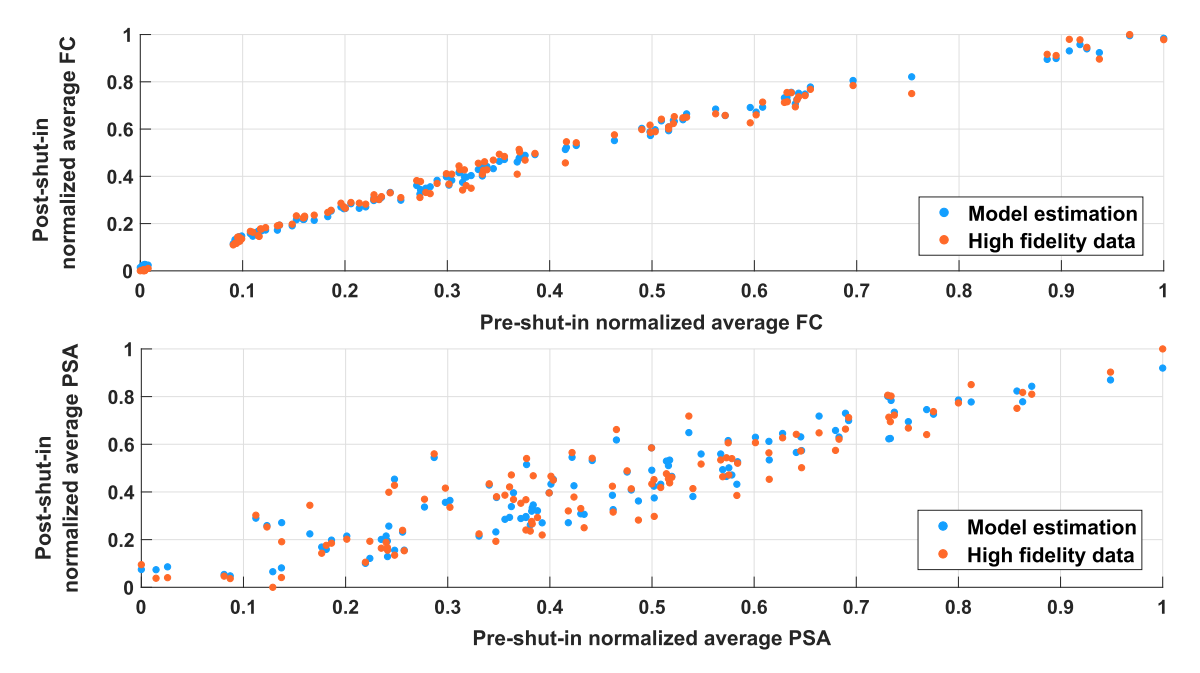


Fig. 10. Scatter graph for training data used in Model 2 (ANN).

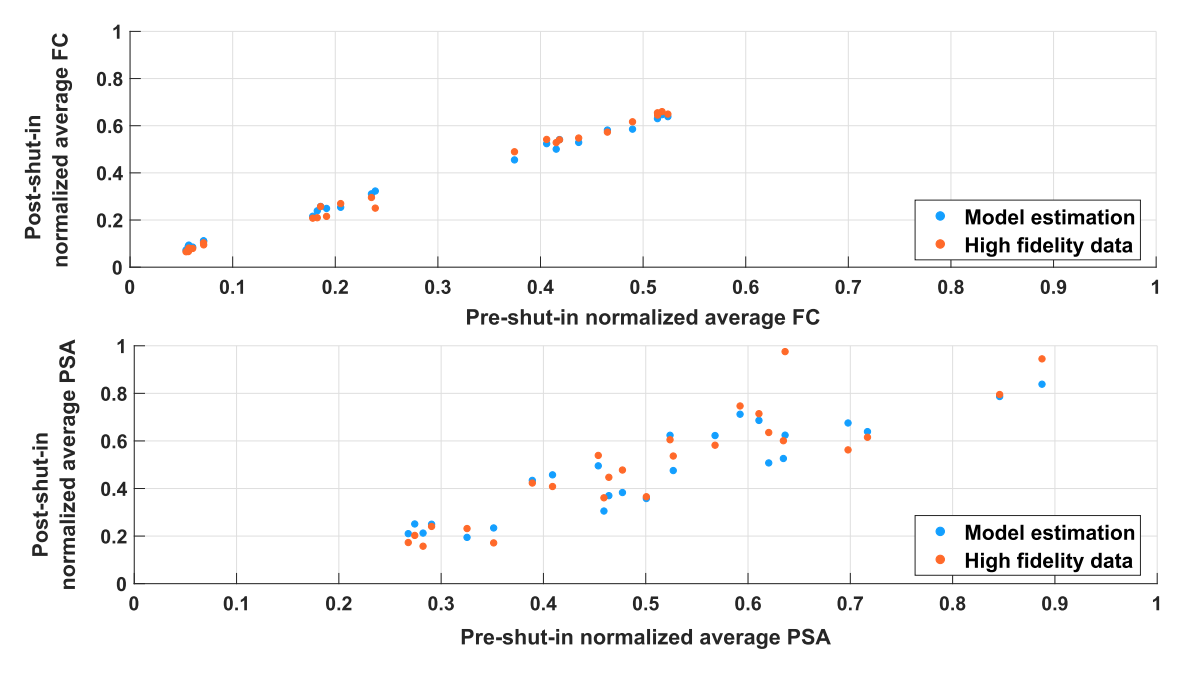


Fig. 11. Scatter graph for validation data used in Model 2 (ANN).

optimization problem to find a maximum in this region for a given amount of proppant to be injected, thereby corresponding to the case of maximum cumulative shale gas production at the end of 10 years.

5. Formulation of optimization strategy using SIMS to maximize shale gas production in unconventional reservoirs

One of the first attempts to design a pumping schedule was done by Nolte (1986), where he developed a power-law type proppant concentration schedule. Despite being quite popular among researchers in academia as well as oil and gas industry since then, it has a few pragmatic restrictions: (1) it does not consider gravity-induced settling of the proppant; (2) it is only applicable to treatments leading to a single hydraulic fracture; (3) a plant-model mismatch might lead to premature

stopping of the hydraulic fracture propagation; and (4) the pumping schedule is designed offline and applied in an open-loop manner to the hydraulic fracturing process.

Gu and Desroches (2003) developed a pumping schedule generator using an iterative method to obtain the desired fracture length and proppant concentration (inverse problem) considering pre-mature bridging and tip screenout. Another approach by Phatak et al. (2013) studied the impact of fracturing fluid volume, proppant size, pumping rate, proppant concentration and proppant injection sequence on shale gas production rate. Later, Dontsov and Peirce (2014) proposed a pumping schedule that has higher accuracy than Nolte (1986) by assuming a weak impact of proppant particles on fracture propagation. However, they did not consider the impact of average PSA and average FC on shale gas production. Recently, a new model-based controller was

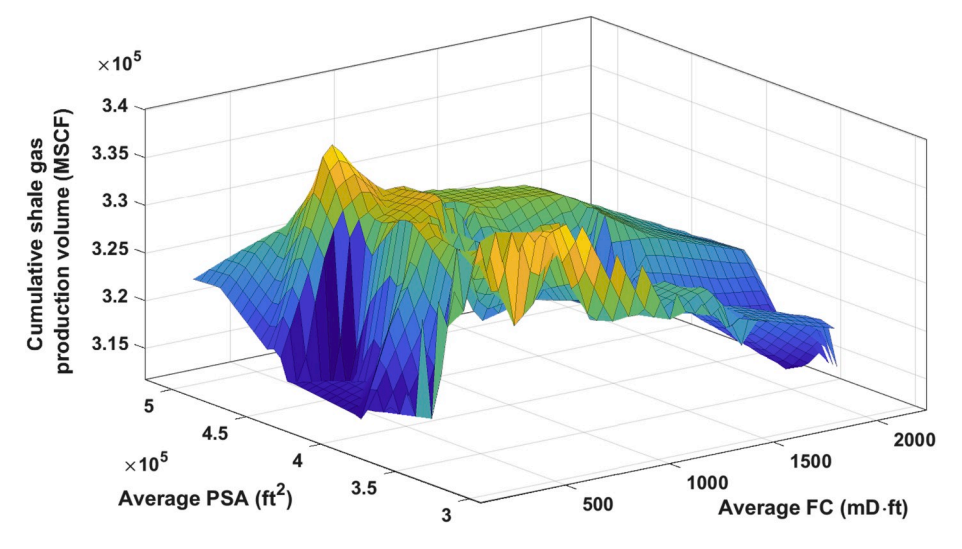


Fig. 12. Illustration of Model 3 in the SIMS framework.

designed by Siddhamshetty et al. (2019) to compute fracturing fluid pumping schedules online and to achieve an optimal fracture geometry by achieving a uniform proppant bank distribution at the end of pumping. They considered multiple simultaneously propagating fractures, and included stress shadow effects and proppant transport as well. Siddhamshetty et al. (2020) further developed this approach for application to naturally fractured unconventional reservoirs. Specifically, in addition to proppant transport, stress shadow effects and simultaneously propagating multiple fractures, Siddhamshetty et al. (2020) also included the presence of natural fractures and their interaction with the propagating hydraulic fractures, and developed a feedback control strategy to maximize the TFSA of the fracture network. However, they only considered the injection of a single-size proppant throughout the stages in their pumping schedule, and did not consider the effect of average PSA and average FC together on the shale oil and gas production.

In this work, we propose a multi-size proppant pumping schedule for simultaneously propagating multiple fractures. We assume the available proppant sizes to be restricted to three diameters- 0.0065 inch, 0.01 inch and 0.02 inch. As shown in the previous sections, since the inclusion of multiple proppant sizes is proposed, the objective can no longer be restricted to just maximizing the TFSA, because of a significant variation in the proppant conductivity across the different proppant sizes. Therefore, to take this variation into account, we propose a pumping schedule that maximizes shale gas production volume, which is a function of average PSA and average FC (Section 4). The SIMS

framework proposed in Section 4 has been integrated within the proposed optimizer to compute a multi-size proppant pumping schedule to maximize cumulative shale gas production volume at the end of 10 years in an unconventional reservoir.

The following optimization problem was solved to compute the optimal pumping schedule:

$$\max_{\substack{C_{stage,1}, \dots, C_{stage,8} \\ Q_{stage,1}, \dots, Q_{stage,8} \\ D_{stage,1}, \dots, D_{stage,8}}} Gas_{frac}\left(C_{stage,m}, Q_{stage,m}, D_{stage,m}\right) \tag{9a}$$

$$C_{stage,m-1} \le C_{stage,m} \le 5 \text{ PPA}$$
 (9e)

$$Q_{min} \le Q_{stage,m} \le Q_{max} \tag{9f}$$

$$D_{stage,m} \in \{0.0065 \text{ inch}, 0.01 \text{ inch}, 0.02 \text{ inch}\}$$
 (9g)

$$m=1,\ldots,8\tag{9h}$$

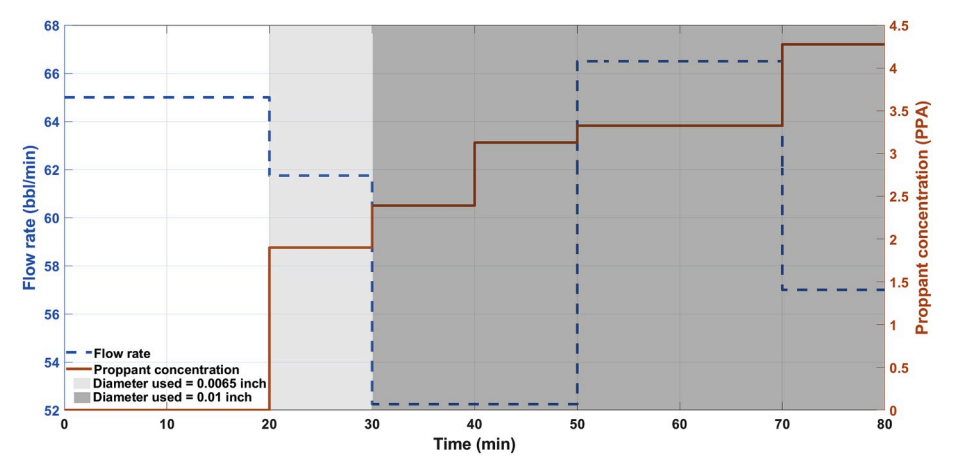


Fig. 13. The pumping schedule obtained from the optimizer, Eq. (9), for Case A.

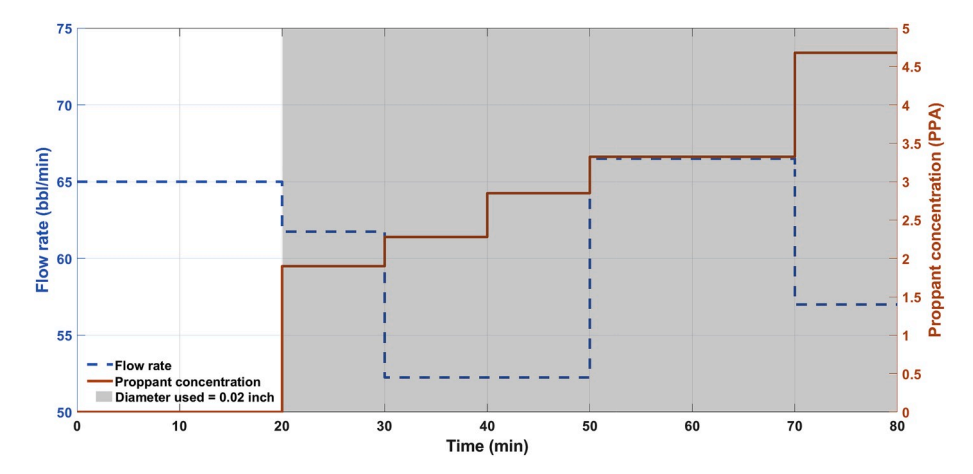


Fig. 14. The pumping schedule obtained from the optimizer, Eq. (9), for Case B.

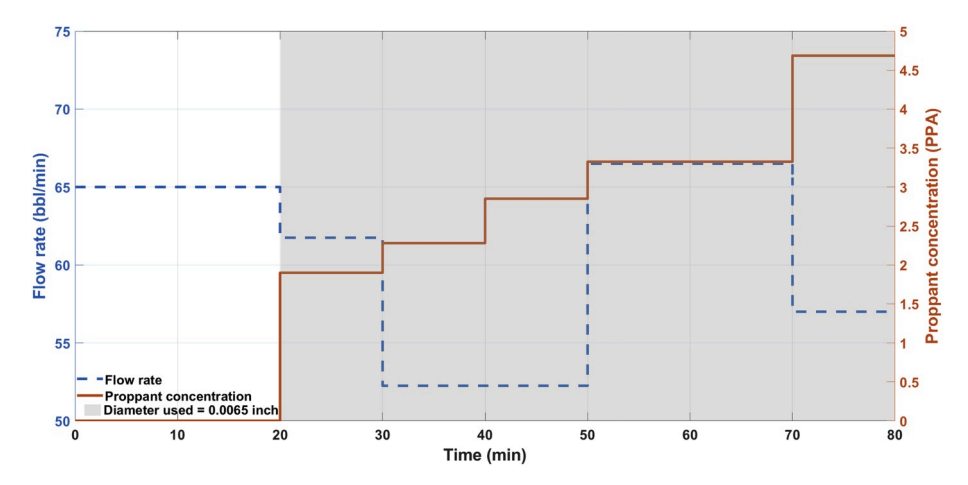


Fig. 15. The pumping schedule obtained from the optimizer, Eq. (9), for Case C.

$$\Delta \left(\sum_{m=1}^{8} Q_{stage,m} C_{stage,m} \right) = M_{prop}$$
(9i)

where Δ denotes the duration of each sampling time, Gas_{frac} is the cumulative volume of shale gas produced at the end of 10 years, the decision variables $C_{stage,m}$, $Q_{stage,m}$ and $D_{stage,m}$ are the concentration, flow rate and the diameter of the injected proppant at the m^{th} stage, respectively. Throughout this work, we assume pumping schedules to have a total of 8 pumping stages, each of 10 mins duration.

In the optimization problem of Eq. (9), Eqs. (9e)-(9h) are the constraints on the decision variables (i.e. fracturing fluid flow rate injected at the wellbore, proppant concentration, and diameter of the proppant). The proppant diameters are chosen in a non-decreasing. The units of fracturing fluid flow rate, proppant concentration and proppant diameter are bbl/min, PPA (1 pound of the proppant added to one gallon of fracturing fluid) and inch, respectively. The total amount of proppant injected is equal to 400,000 lb, constrained using Eq. (9i). The optimization problem has been solved for the following three cases. In Case A, the optimization problem was solved using all the three models of the SIMS framework. In Case B, we assume a 'conductivity-specific' reservoir treatment, where the optimization objective is only to maximize the post-shut-in average FC of the reservoir. Thus, this would require only the first two models of the SIMS framework. In Case C, we assume a 'surface area-specific' reservoir treatment, where the optimization objective is only to maximize the post-shut-in average PSA. Similar to Case B, this would also require only the first two models of the SIMS framework.

Table 1Simulation results after applying the output obtained from the optimizer, Eq. (9), to the high-fidelity model described in Section 2.

Optimization Case	Average PSA (ft ²)	Average FC (mD·ft)	Cumulative shale gas production volume (MSCF)
A	355,398	679	330,036
В	314,789	1983	317,263
C	409,035	181	316,059

Remark 2. Since average PSA and average FC values can be approximately obtained at the end of pumping which typically takes a few hours, such an optimization approach that considers the dependence of the cumulative shale gas production volume on these parameters of practical importance is justified (Zhang et al., 2015; Roshan et al., 2016). Therefore, the optimization strategies proposed in this work are realistic in their applicability.

Remark 3. This work proposes three optimization approaches involving the dependence of cumulative shale gas production volume on the average PSA and average FC, which are two important parameters that determine the cumulative shale gas production from an unconventional reservoir (Wahl, 1965; Ramurthy et al., 2011; Schmidt et al., 2014). However, it is worthwhile to note that there are no optimization strategies currently available in the literature that use important parameters like average PSA and average FC to maximize cumulative shale gas production volume using multi-size proppant pumping schedules.

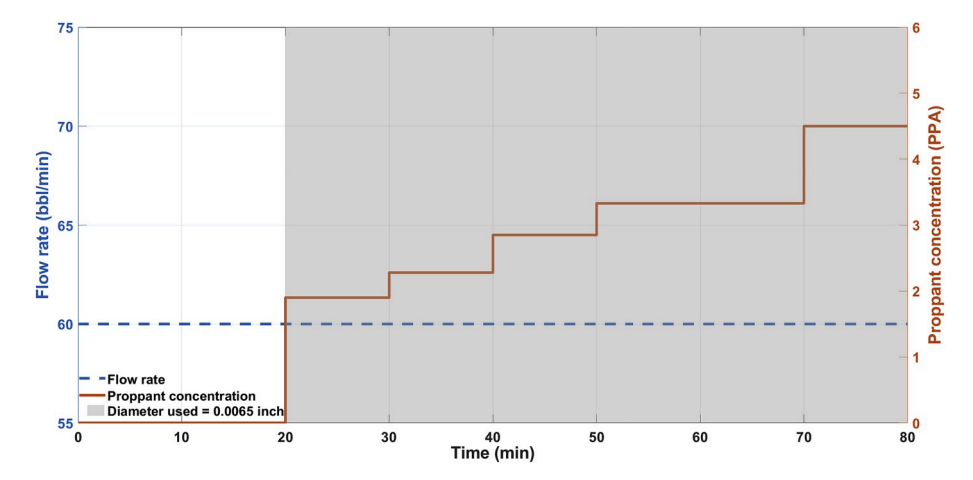


Fig. 16. Nolte's pumping schedule used in this work.

Table 2Comparison of average PSA, average FC, cumulative shale gas production volume from Case A and Nolte's pumping schedule.

Pumping schedule	Average PSA (ft ²)	Average FC (mD·ft)	Cumulative shale gas production volume (MSCF)
Case A	355,398	679	330,036
Nolte (1986)	439,377	190	311,896

6. Optimization results under the proposed framework

In this section, we present optimization results to signify the performance of our proposed optimizer using the SIMS framework developed in Section 4. Mangrove, described in Section 2, has been used as a high-fidelity simulator for a hydraulic fracturing operation resulting in simultaneously propagating multiple fractures.

6.1. Optimization results for case studies

In Case A, the total proppant amount considered is $M_{prop}=400000~\mathrm{lb}$. Using the three models incorporated in the SIMS framework, the proposed optimizer in Section 5 computed the pumping schedule to maximize the cumulative shale gas production volume, 10 years after initiation of the hydraulic fracturing operation. The pumping schedule obtained from the optimizer is shown in Fig. 13. When this pumping schedule was applied to the high-fidelity model, the average PSA and average FC values obtained were 355,398 ft2 and 679 mD· ft, respectively. The cumulative gas production volume at the end of 10 years was 330,036 MSCF. In Case B, the total proppant amount considered is $M_{prop} = 400000$ lb. However, since the objective was chosen to maximize the average FC of the propped fractures, only Model 1 and Model 2 of the SIMS framework were incorporated into the optimization problem, Eq. (9). For this case, the pumping schedule obtained is shown in Fig. 14. When this pumping schedule was applied to the high-fidelity model, the average PSA and average FC values were 314,789 ft² and 1983 mD·ft, respectively. The cumulative shale gas production volume at the end of 10 years was 317,263 MSCF. In Case C, we assumed a total proppant amount of $M_{prop} = 400000$ lb , similar to Case A and Case B. Since the objective was chosen to maximize the average PSA of the propped fractures, we included only Model 1 and Model 2 into the optimizer, Eq. (9). For this case, the pumping schedule obtained is shown in Fig. 15. When this pumping schedule was applied to the highfidelity model, the average PSA and average FC values were 409,035 ft² and 181 mD·ft, respectively. The cumulative gas production volume at the end of 10 years was 316,059 MSCF.

Table 1 summarizes the results obtained after solving the

optimization problem, Eq. (9). The pumping schedule obtained in Case A maximizes the cumulative shale gas production volume for a general case, where the effect of average PSA and average FC is coupled. We have also presented two other cases that provide pumping schedules aimed at maximizing cumulative shale gas production volume by either considering average FC or average PSA separately. From the pumping schedule results, we can clearly see that average FC is maximized in Case B, when all the stages in the pumping schedule have the largest proppant (i.e., 0.02 inch). Meanwhile, the average PSA is maximized in Case C, when the smallest proppant (i.e., 0.0065 inch) is injected throughout the pumping schedule. However, Case A, where average PSA and average FC are considered together, gives the maximum cumulative shale gas production volume in an unconventional reservoir considering simultaneously propagating multiple fractures. These results are in agreement with the analysis presented in Section 3.

Remark 4. Please note that in this work, MATLAB fmincon was used to obtain a local solution of the proposed optimization problem. The optimization problem has been initialized and solved for random initial conditions. In all the numerical experiments, the solution converged to the reported value giving the local optimum. However, global optimization analysis has not been conducted for simplicity, and is deemed to be outside the scope of this work.

6.2. Comparison with existing work

In this work, we have used Nolte's pumping schedule described in Section 5 for comparison with the output of the proposed optimizer. The pumping schedule is shown in Fig. 16.

This pumping schedule was applied to the high-fidelity model and the results obtained were compared with Case A, as shown in Table 2.

From the results, we can see that the pumping schedule obtained from Case A, Eq. (9), gives a cumulative shale gas production volume more than that of Nolte's schedule.

All the calculations, including model training, validation and deployment in the optimization problem were facilitated using MATLAB R2018b on a Dell workstation, powered by Intel(R) Core(TM) i7-4790 CPU@3.60GHz, running on the Windows 10 OS.

7. Conclusions

In this work, we designed a multi-size proppant pumping schedule for the case of simultaneously propagating multiple fractures to maximize cumulative shale gas production volume from unconventional reservoirs. From the sensitivity analysis, we found out that the pumping schedule used for hydraulic fracturing determines the average PSA and average FC of the propped fractures, which in-turn are two useful parameters that determine the cumulative shale gas production volume

from an unconventional reservoir. We also found out that smalldiameter proppant resulted in lower average FC and higher average PSA, whereas large-diameter proppant resulted in higher average FC and lower average PSA. Therefore, we developed SIMS, a framework that links the pumping schedule parameters to the cumulative gas production volume. In this framework, we first developed a MOESP-based ROM to accurately represent the fracturing process. Then, an ANN was trained and tested to model the proppant settling process. The final model developed in SIMS is a map that was generated using the reservoir simulator to obtain the cumulative shale gas produced at the end of 10 years using the average PSA and average FC for an unconventional reservoir. Finally, we proposed a framework to maximize the cumulative shale gas production volume by computing pumping schedules (i.e., flow rate, proppant concentration, and proppant diameter at the wellbore) using offline optimization techniques. Simulation results presented in this work include the pumping schedules obtained from the optimizer for three different case studies. From the results obtained for these three case studies, we found out that the cumulative shale gas production volume obtained at the end of 10 years was maximized in Case A, when the pumping schedule included varying proppant diameters across the pumping stages. When the pumping schedule obtained in Case A was compared with the pumping schedules obtained in Case B, Case C and Nolte's schedule, the proposed method was found to increase the cumulative shale gas production volume by 4.03%, 4.42% and 5.82%, respectively.

Declaration of competing interest

The authors declare that they have no known competing financial interests or personal relationships that could have appeared to influence the work reported in this paper.

Acknowledgements

The authors gratefully acknowledge financial support from the National Science Foundation (CBET-1804407), the Department of Energy (DE-EE0007888-10-8), the Texas A&M Energy Institute, and the Artie McFerrin Department of Chemical Engineering.

Appendix A. Supplementary data

Supplementary data to this article can be found online at https://doi.org/10.1016/j.jngse.2020.103349.

References

- Cipolla, C.L., Fitzpatrick, T., Williams, M.J., Ganguly, U.K., 2011. Seismic-to-simulation for unconventional reservoir development. In: SPE Reservoir Characterisation and Simulation Conference and Exhibition (SPE 146876), Abu Dhabi, UAE.
- Crouch, S.L., Starfield, A.M., Rizzo, F.J., 1983. Boundary element methods in solid mechanics. J. Appl. Mech. 50, 704.
- Daneshy, A., 1978. Numerical solution of sand transport in hydraulic fracturing. J. Petrol. Technol. 30, 132–140.
- Dontsov, E.V., Peirce, A.P., 2014. A new technique for proppant schedule design. Hydraulic Fracturing Journal 1, 1–8.
- Fredd, C., McConnell, S., Boney, C., England, K., 2000. Experimental study of hydraulic fracture conductivity demonstrates the benefits of using proppants. In: SPE Rocky Mountain Regional/Low-Permeability Reservoirs Symposium and Exhibition (SPE 60326), Denver, CO.
- Gu, H., Desroches, J., 2003. New pump schedule generator for hydraulic fracturing treatment design. In: SPE Latin American and Caribbean Petroleum Engineering Conference, Port-of-Spain, Trinidad and Tobago.
- Gu, Q., Hoo, K.A., 2014. Evaluating the performance of a fracturing treatment design. Ind. Eng. Chem. Res. 53, 10491–10503.

- Hu, X., Wu, K., Li, G., Tang, J., Shen, Z., 2018. Effect of proppant addition schedule on the proppant distribution in a straight fracture for slickwater treatment. J. Petrol. Sci. Eng. 167, 110–119.
- Mack, M.G., Elbel, J.L., Piggott, A.R., 1992. Numerical representation of multilayer hydraulic fracturing. In: The 33th US Symposium on Rock Mechanics (ARMA-92-0335), Santa Fe, NM.
- Narasingam, A., Kwon, J.S., 2017. Development of local dynamic mode decomposition with control: application to model predictive control of hydraulic fracturing. Comput. Chem. Eng. 106, 501–511.
- Narasingam, A., Kwon, J.S., 2018. Data-driven identification of interpretable reducedorder models using sparse regression. Comput. Chem. Eng. 119, 101–111.
- Narasingam, A., Siddhamshetty, P., Kwon, J.S., 2017. Temporal clustering for order reduction of nonlinear parabolic PDE systems with time-dependent spatial domains: application to a hydraulic fracturing process. AIChE J. 63, 3818–3831.
- Narasingam, A., Siddhamshetty, P., Kwon, J.S., 2018. Handling spatial heterogeneity in reservoir parameters using proper orthogonal decomposition based ensemble kalman filter for model-based feedback control of hydraulic fracturing. Ind. Eng. Chem. Res. 57, 3977–3989.
- Nolte, K.G., 1986. Determination of proppant and fluid schedules from fracturingpressure decline. SPE Prod. Eng. 1, 255–265.
- Olson, J.E., 2008. Multi-fracture propagation modeling: applications to hydraulic fracturing in shales and tight gas sands. In: The 42nd US Symposium on Rock Mechanics (ARMA-08-327), San Francisco, CA.
- Phatak, A., Kresse, O., Nevvonen, O.V., Abad, C., Cohen, C.e., Lafitte, V., Abivin, P., Weng, X., England, K.W., 2013. Optimum fluid and proppant selection for hydraulic fracturing in shale gas reservoirs: a parametric study based on fracturing-toproduction simulations. In: SPE Hydraulic Fracturing Technology Conference (SPE 163876), the Woodlands, TX.
- Ramurthy, M., Barree, R.D., Kundert, D.P., Petre, J.E., Mullen, M.J., 2011. Surface-area vs. conductivity-type fracture treatments in shale reservoirs. In: SPE Hydraulic Fracturing Technology Conference, the Woodlands, TX.
- Roshan, H., Sarmadivaleh, M., Iglauer, S., 2016. Shale fracture surface area measured by tracking exchangeable cations. J. Petrol. Sci. Eng. 138, 97–103.
- Schiller, L., Naumann, A., 1935. A drag coefficient correlation. VDI Zeitung 77, 318–320.
 Schmidt, D., Rankin, P.R., Williams, B., Palisch, T., Kullman, J., 2014. Performance of mixed proppant sizes. In: SPE Hydraulic Fracturing Technology Conference (SPE 168629). the Woodlands. TX.
- Siddhamshetty, P., Bhandakkar, P., Kwon, J.S., 2020. Enhancing total fracture surface area in naturally fractured unconventional reservoirs via model predictive control. J. Petrol. Sci. Eng. 184, 106525.
- Siddhamshetty, P., Kwon, J.S., 2019. Simultaneous measurement uncertainty reduction and proppant bank height control of hydraulic fracturing. Comput. Chem. Eng. 127, 272–281
- Siddhamshetty, P., Liu, S., Valkó, P.P., Kwon, J.S., 2017. Feedback control of proppant bank heights during hydraulic fracturing for enhanced productivity in shale formations. AIChE J. 64, 1638–1650.
- Siddhamshetty, P., Wu, K., Kwon, J.S., 2018a. Optimization of simultaneously propagating multiple fractures in hydraulic fracturing to achieve uniform growth using data-based model reduction. Chem. Eng. Res. Des. 136, 675–686.
- using data-based model reduction. Chem. Eng. Res. Des. 136, 675–686. Siddhamshetty, P., Wu, K., Kwon, J.S., 2019. Modeling and control of proppant distribution of multi-stage hydraulic fracturing in horizontal shale wells. Ind. Eng. Chem. Res. 58, 3159–3169.
- Siddhamshetty, P., Yang, S., Kwon, J.S., 2018b. Modeling of hydraulic fracturing and designing of online pumping schedules to achieve uniform proppant concentration in conventional oil reservoirs. Comput. Chem. Eng. 114, 306–317.
- Sidhu, H.S., Narasingam, A., Siddhamshetty, P., Kwon, J.S., 2018a. Model order reduction of nonlinear parabolic PDE systems with moving boundaries using sparse proper orthogonal decomposition: application to hydraulic fracturing. Comput. Chem. Eng. 112, 92–100.
- Sidhu, H.S., Siddhamshetty, P., Kwon, J.S., 2018b. Approximate dynamic programming based control of proppant concentration in hydraulic fracturing. Mathematics 6, 122
- Wahl, H.A., 1965. Horizontal fracture design based on propped fracture area. J. Petrol. Technol. 17, 723–730.
- Weng, X., Kresse, O., Chuprakov, D., Cohen, C.E., Prioul, R., Ganguly, U., 2014. Applying complex fracture model and integrated workflow in unconventional reservoirs. J. Petrol. Sci. Eng. 124, 468–483.
- Westwood, R.F., Toon, S.M., Cassidy, N.J., 2017. A sensitivity analysis of the effect of pumping parameters on hydraulic fracture networks and local stresses during shale gas operations. Fuel 203, 843–852.
- Yang, S., Siddhamshetty, P., Kwon, J.S., 2017. Optimal pumping schedule design to achieve a uniform proppant concentration level in hydraulic fracturing. Comput. Chem. Eng. 101, 138–147.
- Zhang, J., Kamenov, A., Zhu, D., Hill, A., 2015. Development of new testing procedures to measure propped fracture conductivity considering water damage in clay-rich shale reservoirs: an example of the barnett shale. J. Petrol. Sci. Eng. 135, 352–359.